Proc. of the 8th International Symposium on Geotechnical Safety and Risk (ISGSR)
Edited by Jinsong Huang, D.V. Griffiths, Shui-Hua Jiang, Anna Giacomini and Richard Kelly
 Published by Research Publishing, Singapore.
doi: 10.3850/978-981-18-5182-7_01-009-cd

Three-Parameter Lognormal Distribution to Estimate Ultimate Bearing Capacity of Pile Foundations with Extrapolation of Load-Settlement Curves

Naoki Suzuki[1]

[1]IPA Support Department, GIKEN LTD., Tokyo, Japan.
E-mail: suzuki.n@giken.com

Abstract: The bearing capacity of piles has a large variability when estimated from prior geotechnical investigation alone. On-site tests are effective in geotechnical risk management, particularly for ground whose performance is not well known and/or for new piling methods. The authors have been attempting to develop simple static load tests with press-in piles. However, there are issues in estimating the ultimate bearing capacity; (1) it is difficult to apply a large load owing to the limitation of piling machines and reaction piles; (2) excessive load may affect the performance of piles. Thus, there is an urgent need for a method to extrapolate load-settlement curves and estimate ultimate capacity. Accordingly, we investigated the relationship between the measured ultimate capacity, the estimated ultimate capacity by Chin's extrapolation, and the maximum load used for the estimation, based on a database of pile load tests. It was found that the ratio of the measured load to the estimated one follows a three-parameter (TP) lognormal distribution well with the maximum load as the lower bound. Moreover, the effect of the TP lognormal distribution on the reliability of the structure is modeled and discussed.

Keywords: pile foundation; bearing capacity; probability distribution; load-settlement curve; reliability-based design.

1 Introduction

In-situ verification of pile bearing capacity remains an effective tool against geotechnical risk because there is relatively large variability when the capacity is estimated from prior ground investigation alone, particularly for unusual ground types (e.g., rock layers) and new piling methods where the performance is not well known.

The authors are investigating a method to assess the pile capacity by simply pressing piles, which can be easily applied for all piles after installation (Suzuki and Ishihara, 2019). However, there are some considerable issues in confirming the ultimate capacity; (1) it is difficult to apply a large load owing to the limitation of construction machines and reaction piles; (2) an excessive loading history may affect the performance of piles. Therefore, extrapolation of the incomplete load-settlement curve is required to estimate the ultimate load.

Numerous researchers have proposed and evaluated methods for the extrapolation of the load-settlement curve. Galbraith et al. (2014) summarized the variability of the estimation and the settlement normalized by the pile diameter for Chin's extrapolation method (Chin 1972), and the authors reported that the coefficient of variation (COV) of the estimation decreases as the settlement increases. However, in addition to the settlement, the maximum load of the test can be a critical piece of information in the data of loading tests.

In this study, we extrapolated load-settlement curves using Chin's method and estimated ultimate capacities based on the FHWA database. Moreover, we investigated the probability distribution of the estimation error of the extrapolated capacity and found that a three-parameter (TP) lognormal distribution fits it well. Lastly, we examined the effect on the reliability of the structure based on parametric studies.

2 Extrapolation Curves and Database of Pile Load Tests

Hyperbolic approximation using Chin's method uses only two parameters (Eq. 1) and is often employed to extrapolate the load-settlement curve of a pile was applied in this study (Figure 1). It was omitted due to limitations of paper space; however, it was found that the formulae derived by Chin, Van Der Veen (1957), Hansen, Uto et al. (1982), and Zhang and Zhang (2012) did not exhibit a significant difference in the extrapolation variation. Each method has been explained and described by Fellenius and Rahman (2019), except for Uto et al. (1982), which represented the load-settlement curve with cumulative distribution function (CDF) for the Weibull distribution.

$$Q_n = Q_u \frac{S_n}{S_n + S_y} \tag{1}$$

where Q_u=ultimate capacity, S_y=characteristic settlement, Q_n=capacity, S_n=settlement.

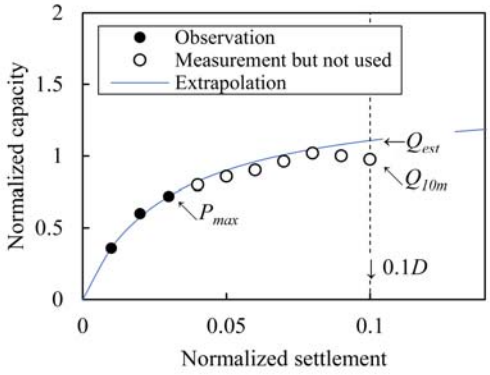

Figure 1. Illustration of the load-settlement curves and the extrapolation.

In total, 129 load-settlement curves of static push-in tests were used in FHWA Deep Foundation Load Test Database (DFLTD) version 2.0 (e.g., Petek et al. 2016; Kalavar and Ealy 2000) under the following conditions; the ultimate bearing capacity is observed directly; the number of measurement points is sufficient for extrapolations, and the type of the piling methods is either drilled shafts or impact-driven piles. The ultimate bearing capacity, Q_{10}, is defined as that when the pile head settles down at 10% of the pile diameter, D.

Figure 2a illustrates the relationship between measured ultimate bearing capacity, Q_{10m}, and maximum loads, P_{max}, both normalized by the estimated capacity, Q_{est}. Accordingly, each curve is fitted using only the data whose capacity is under the maximum loads based on the least square method. The line y=1.0 indicates Q_{est}=Q_{10m}, and the line x=y indicates P_{max}=Q_{10m}. Although some of the ultimate capacities of the open-ended impact driven piles became lower than those of the maximum load (indicating the case where the capacity softens as the piles settle downs), there were no differences between pile types. Based on the sufficiently small number of softened specimens, it can be inferred that the maximum load plays a role in the lower bound. Moreover, since all the observed data were used equally in fitting the curves, the ratio of measured to estimated capacities, Q_{10m}/Q_{est}, does not converge to 1.0 at P_{max}/Q_{est}. Accordingly, some techniques could be considered, such as thinning the data appropriately or weighting the observations (e.g., Nakatani et al., 2009).

Figure 2b depicts the sample mean and COV of the ratio, Q_{10m}/Q_{est}, in a moving window of size 0.1. In this study, only data within $\pm 3\sigma$ of the mean were used in the calculation of the mean and COV to exclude outliers. When the maximum load exceeded 30% of the estimated capacity, the estimated value shows good agreement with the measured value. Meanwhile, when the maximum load is smaller, the capacity is overestimated to the measured value. In general, the COVs are in good agreement with those reported by Matsuo et al. (1989). The

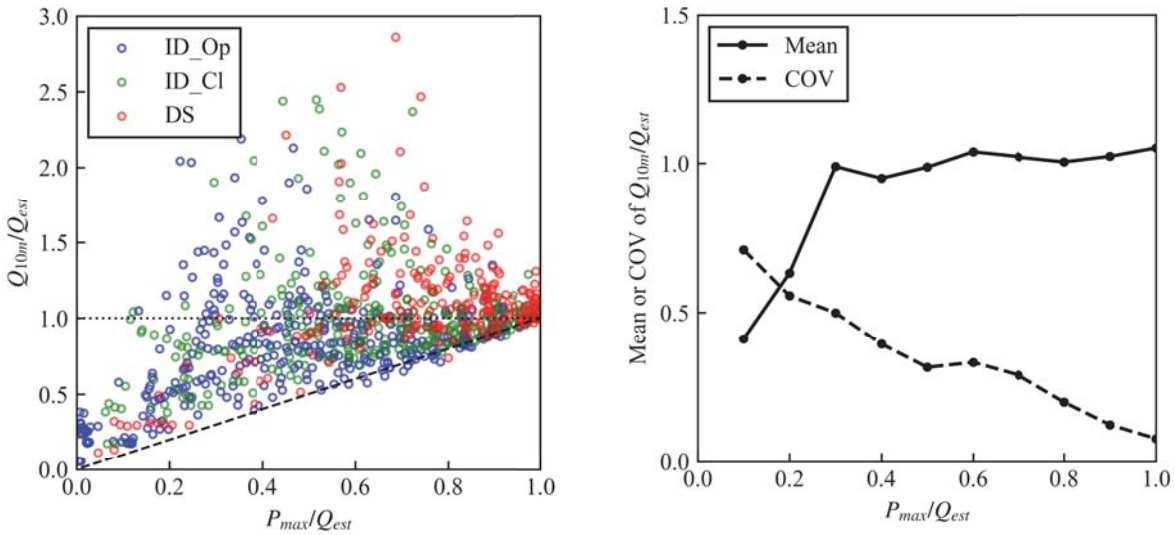

(a) Scatters of ultimate bearing capacity and the estimation by Chin's extrapolation.

(b) Sample mean and COV in the moving window of size 0.1.

Figure 2. Variation of ultimate bearing capacity estimation using Chin's extrapolation in relation to maximum load. ID_Op= open-ended impact-driven piles, ID_Cl= closed-ended impact-driven piles, and DS=drilled shafts. The number of piles is ID_Op: 27, ID_Cl: 46, DS: 56, respectively.

authors reported that the error in the estimation of ultimate capacity using Weibull formula had about 34% of COV at 40-60% loading level and about 6% at more than 90% loading level, though the reported loading level was defined as the ratio P_{max}/Q_{10m}, not P_{max}/Q_{est}.

Figure 3 shows the histogram of Q_{10m}/Q_{est} at P_{max}/Q_{est}□0.7 with fitting curves of ordinary lognormal, TP lognormal, and truncated (TC) lognormal distributions. The distributions were fitted using the maximum likelihood estimation method. The probability density function (PDF) of TP lognormal is as follows:

$$f\left(x;m,s,\delta\right)=\frac{1}{s\left(x-\delta\right)\sqrt{2\pi}}\exp\left[-\frac{\left(\ln\left(x-\delta\right)-m\right)^2}{2s^2}\right],\left(x>\delta\right) \tag{2}$$

where m indicates bias, s denotes a scale parameter, and δ refers to the lower bound (also called location). The ordinary lognormal distribution function is Eq. 2 with δ=0. The TC lognormal function is the ordinary lognormal PDF that becomes zero when the value is less than δ and adjusted so that the sum of the probability densities becomes one with reference to Najjar and Gilbert (2009). Both TP and TC lognormal distribution naturally have a well-fitted lower hem, whereas TC does not have a well-fitted upper hem as well as ordinary lognormal.

Table 1 lists the results of Akaike information criterion (AIC) (Akaike 1973) and the best fitted functions. AIC = -2ln$L$ + 2k, where k denotes the number of estimated parameters, and L denotes the maximum value of the likelihood function for the model.

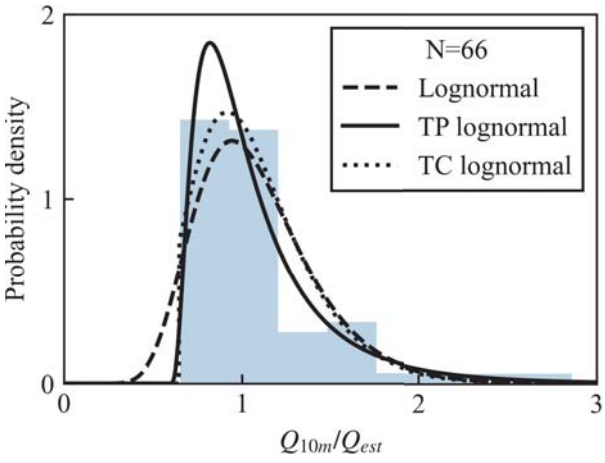

Figure 3. Statistics of ultimate bearing capacity estimation using Chin's extrapolation method. P_{max}/Q_{est}□0.7

Table 1. AIC of fitting lognormal functions.

P_{max}/Q_{est}	Sample	Ordinary logn.	TP logn.	TC logn.
0.3	36	35.0	36.8	37.0
0.4	42	31.1	33.0	33.1
0.5	50	30.6	27.5	31.8
0.6	59	10.6	4.4	8.4
0.7	66	40.2	25.5	32.9
0.8	47	-31.7	-34.6	-17.7
0.9	84	-97.1	-115.7	-95.1

Note: Bold indicates the minimum AIC in three candidate distributions. TP=three parameter, TC=truncated, logn.=lognormal

When P_{max}/Q_{est} is higher than 0.4, TP lognormal distribution is better fitted than others. While P_{max}/Q_{est} is less than 0.5, the differences are minimal. Moreover, the ordinary/TP lognormal functions are easily used by computing modules, such as scipy in python (Scipy community, n.d.), and these would be appropriate for the model.

3 Mathematical Formulation for Reliability

In this section, the reliability index, β, is introduced based on the TP lognormal distribution. Here, if the random variable X with mean μ_X and variance σ_X^2 follows a lognormal distribution $\Lambda(m_X, s_X^2)$ with lower bound, δ_X, the parameters have the relations expressed in Eqs. 3 and 4.

$$m_X=\ln\left(\mu_X-\delta_X\right)-\frac{1}{2}s_X^2 \tag{3}$$

$$s_X=\sqrt{\ln\left[1+\left(\frac{\sigma_X}{\mu_X-\delta_X}\right)^2\right]} \tag{4}$$

Here, failure is defined as the case where the capacity, R, is less than the load, S. The probability of failure is as follows:

$$P_f=\Pr\left(R<S\right)=\int_0^\infty\int_0^\infty\Pr\left(R<S\mid x,y\right)f_R\left(x\right)f_S\left(y\right)dxdy=\Phi\left(-\beta\right) \tag{5}$$

where Φ denotes the cumulative distribution function (CDF) of the standard normal distribution. If R and S follow independent ordinary lognormal distributions (i.e., δ_R=δ_S=0), then the reliability index is expressed by the well-known Eq. 6; however, it is not clear for TP lognormal.

$$\beta_{\log} = \ln\left(\frac{\mu'_R}{\mu'_S}\right) \Bigg/ \sqrt{\ln\left[\left(1+\left(\frac{\sigma_R}{\mu_R}\right)^2\right)\left(1+\left(\frac{\sigma_S}{\mu_S}\right)^2\right)\right]} \tag{6}$$

$$\mu'_X = \delta_X + \exp\left(m_X\right) \tag{7}$$

When R and S follow independent TP lognormal distributions, the reliability index can be introduced using the normalization as follows. First, R and S are transformed into x and y which follow the standard normal distribution, respectively. The line R=S is also transformed in coordinates into the curve, Eq. 9.

$$x = \frac{\ln\left(X-\delta_X\right)}{s_X} - m_X \tag{8}$$

$$y = \frac{\ln\left[\exp\left(\left(x+m_R\right)s_R\right)+\delta_R-\delta_S\right]}{s_S} - m_S \tag{9}$$

If R and S are independent, the point with the reliability index, β, has the minimum graphical distance from the origin O to the curve R=S. If a minimum distance exists, then it is denoted by C(x_f, y_f), then the curve R=S and the line OC are orthogonal at point C.

$$\frac{dy}{dx} = \frac{s_R}{s_S}\frac{\exp\left(\left(x+m_R\right)s_R\right)}{\exp\left(\left(x+m_R\right)s_R\right)+\delta_R-\delta_S} \tag{10}$$

$$\frac{dy}{dx}\Big|_{x=x_f} \cdot \frac{y_f}{x_f} = -1 \tag{11}$$

A simultaneous equation is used in Eq. 9 to 11, and x_f and y_f are derived. Finally, the reliability index is obtained by substituting them into Eq. 13.

$$\frac{m_S}{x_f} - \frac{\ln\left[\exp\left(\left(x_f+m_R\right)s_R\right)+\delta_R-\delta_S\right]}{x_f s_S} - \frac{s_S}{s_R}\frac{\exp\left(\left(x_f+m_R\right)s_R\right)+\delta_R-\delta_S}{\exp\left(\left(x_f+m_R\right)s_R\right)} = 0 \tag{12}$$

$$\beta_{TP\log} = \sqrt{x_f^2+y_f^2} \tag{13}$$

4 Parametric Study

In this section, the effect of the maximum load of the load test on the reliability is investigated based on parametric studies. The estimation reliability of the extrapolation is a function comprising three parameters: bias, scale, and lower bound. Since the maximum load leads to both an increase in the lower bound and a decrease in scale, the two should be evaluated independently. The case was divided into three aspects: the existence of prior information, the type of COV_Q, and the existence of lower bound (i.e., ordinary or TP lognormal distribution).

For simplicity, it is assumed that the estimated bias always becomes 1.0 when the lower bound increases from 0 to 1.0, and the estimated COV decreases linearly from 0.6 to 0.1 with reference to Figure 2b. However, when the bearing capacity is estimated solely from ground investigations, COV_Q=0.6 is larger than the COV of about 0.3-0.4 (e.g., Yang et al. 2015). Therefore, it is unreasonable to estimate the capacity from the load-settlement curve alone when the mechanism of the bearing capacity is obtained using the ground type and piling method. Therefore, the following two types of prior information are considered; A) the ultimate bearing capacity follows lognormal distribution with a COV_Q of 0.35 and that the mean equals the value estimated from the load-settlement curve; B) there is no prior information for sites with new piling methods or unusual ground conditions.

Table 2. Cases of parametric studies.

Case	Prior information	Type of COV_Q	Lower bound
A1	COV=0.35	Linear (0.6 to 0.1)	Yes
A2		Linear (0.6 to 0.1)	No
A3		Const. (0.6)	Yes
B1	None	Linear (0.6 to 0.1)	Yes
B2		Linear (0.6 to 0.1)	No
B3		Const. (0.6)	Yes

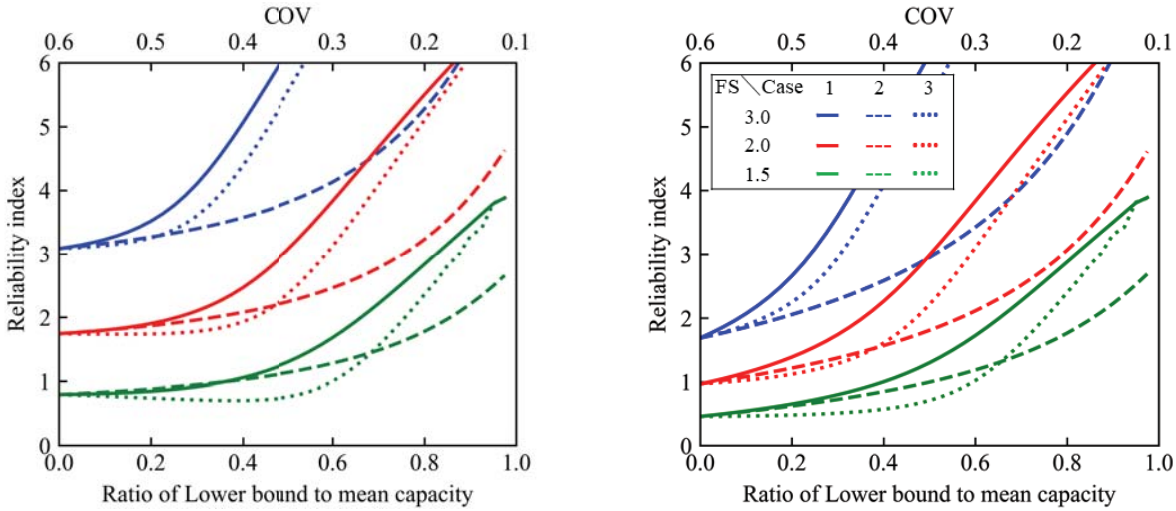

(a) Case A (with prior information) (b) Case B (without prior information)

Figure 4. Effect of loading on the reliability index. The line styles mean simulation cases shown in Table 2.

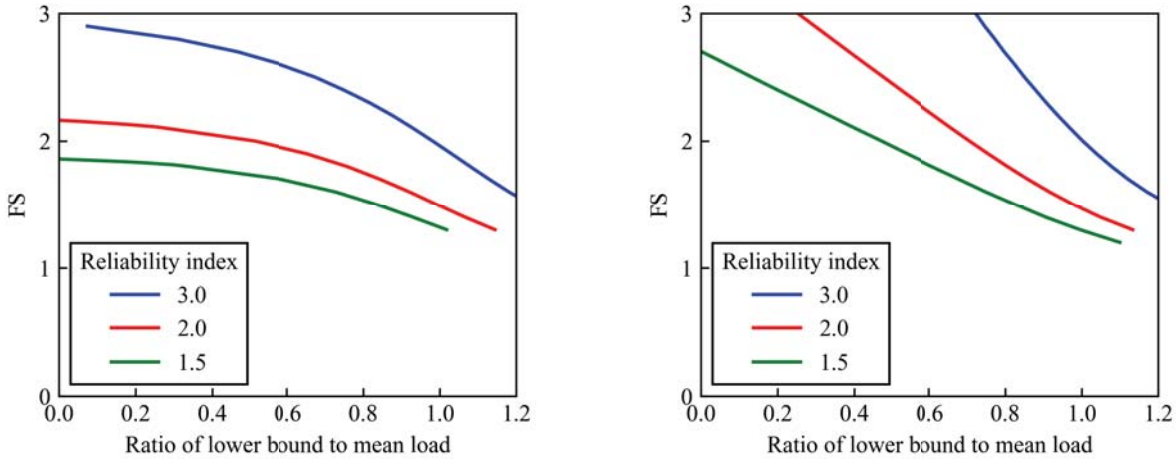

(a) Case A (b) Case B

Figure 5. Application graph of FS and lower bound

Lastly, a total of six cases were simulated by changing the factor of safety (FS) from 1.5 to 3.0 (Table 2). FS is defined as the ratio of the expected ultimate capacity to the expected load at the design stage. The reliability index was numerically calculated using Eq. 5 by dividing the capacity and the load normalized by the mean load into 1000 parts between 0 and 5. Moreover, it was also assumed that the load follows an ordinary lognormal distribution and the bias=1.0 and the COV_S=0.1 with reference to dead load in the previous works, such as Phoon and Kulhawy (1999).

Figure 4 illustrates the effect of the loading level on the reliability index. As the lower bound increases, the reliability index increases monotonically, which is characteristically similar to the results reported by Najjar and Gilbert (2009).

Case A2 (dashed line) indicates the effect of only a decrease of COV_Q and A3 (dotted line) indicates that of lower bound. A2 conformed with A1 at small lower bound and small FS. Initially, A3 was much smaller than A1; however, as lower bound increases, A3 approached A1 asymptotically.

Case B has a smaller β than Case A at small lower bound. However, Case B approaches Case A at large lower bound. It can be stated that even in the case of no prior information, the reliability is equivalent to that

with prior information at a certain load. In addition, the difference between B1 and B2 at FS=2.0 (red lines) appears to be larger than that between A1 and A2.

From the above, it can be stated that Cases 2 and 3 underestimate β in all conditions, and that TP lognormal model is effective, particularly when FS is large, the load is high, and there is no prior information. Noticeably, β of Case A3 (FS=1.5) becomes smaller when the lower bound is in the range of 0.2 to 0.5. It is primarily because the peak of the posterior distribution becomes smaller due to the strong assumption that the expected capacity is the same as that of the prior information and the condition with small FS. The validity of this assumption should be re-examined in the future.

Furthermore, the relationship between FS and the maximum load required to obtain a certain target reliability index is illustrated in Figure 5, based on cases A1 and B1. Note that the x-axis is normalized by the load instead of the capacity. For example, if the maximum load is 0.6 times the expected design load and the target reliability index is 3.0, then the FS is required to be 2.6.

In general, the cost of static load tests is approximately proportional to the maximum load carried, and the cost of construction is proportional to the FS. The maximum load and FS are inversely related to achieve a target reliability index. Therefore, load and FS are tradeoffs that should be considered simultaneously to minimize the total cost. Compared with Figure 5a, the slopes of y to x are more prominent in Figure 5b. Thus, it can be inferred that load tests become a more cost-effective tool in the absence of prior information.

5 Conclusions

In this study, the modeling error of the extrapolation of the load-settlement curve was investigated based on the database of pile loading tests to promote to use the piling data.

- TP lognormal with the maximum load as lower bound fitted well with the results of extrapolated ultimate capacity.
- The maximum load leads to both an increase in the lower bound and a decrease in COV; the former increases the reliability index, particularly at a large lower bound; the latter increases the reliability index at a small lower bound and small FS.
- The application graph of FS and maximum load to achieve the target reliability index has been developed. In particular, in the absence of prior information, the selection of an appropriate FS and maximum load may minimize the construction cost.

References

Akaike, H. (1973). Information theory and an extension of the maximum likelihood principle. *Proceedings of the 2nd International Symposium on Information Theory*, 267–281.

Chin, F. (1972). The inverse slope as a prediction of ultimate bearing capacity of piles. *Proceedings of the 3rd South-East Asian Conference on Soil Engineering*, 83–91.

Fellenius, B. H., & Rahman, M. M. (2019). Load-movement Response by t-z and q-z Functions. *Geotechnical Engineering*, 50(3).

Galbraith, A. P., Farrell, E. R., & Byrne, J. J. (2014). Uncertainty in pile resistance from static load tests database. *Proceedings of the Institution of Civil Engineers - Geotechnical Engineering*, 167(5), 431–446.

Kalavar, S., & Ealy, C. (2000). FHWA deep foundation load test database. *Proceedings of Sessions of Geo-Denver 2000 - New Technological and Design Developments in Deep Foundations,* GSP 100, 288, 192–206.

Matsuo, M., Sugai, M., & Kim, S. (1989). Study of methods for evaluation of bearing capacity of steel pipe piles. *Doboku Gakkai Rombun-Hokokushu/Proceedings of the Japan Society of Civil Engineers*, 406, 3-11 (in Japanese).

Najjar, S. S., & Gilbert, R. B. (2009). Importance of Lower-Bound Capacities in the Design of Deep Foundations. *Journal of Geotechnical and Geoenvironmental Engineering*, 135(7), 890–900.

Nakatani, S., M. Shirato, T. Kouno, Y. Nakamura, T. Nomura, K. Yokomaku, & H. Iochi. (2009). Research on the Stability Verification Method of Road Bridge Foundations in the Performance-Based System. *Technical Note of PWRI*, 4136, (in Japanese).

Petek, K., Mitchell, R., & Ellis, H. (2016). FHWA Deep Foundation Load Test Database Version 2.0 User Manual. FHWA-HRT-17-034. https://doi.org/10.21949/1503647

Phoon, K. K., & Kulhawy, F. H. (1999). Characterization of geotechnical variability. *Canadian Geotechnical Journal*, 36(4), 612–624. https://doi.org/10.1139/t99-038

Scipy community. (n.d.). Scipy. Retrieved February 21, 2022, from https://scipy.org/

Suzuki, N., & Ishihara, Y. (2019). Discussion on the method of estimating the ultimate pile capacity from the load-displacement curve at the end of pressing. *Japan Society of Civil Engineers 2019 Annual Meeting*, *74*(III–21).

Uto, K., Fuyuki, M., & Sakurai, M. (1982). How to organize the results of pile loading tests. *Kisoko*, *10*(9), 21-30 (in Japanese).

Van Der Veen, C. (1957). The Bearing Capacity of a Pile. *Proc. 4 Th ICSMFE*, Vol. 2, 72–75.

Yang, Z., Jardine, R., Guo, W., & Chow, F. (2015). A Comprehensive Database of Tests on Axially Loaded Piles Driven in Sand. *Academic Press.* https://doi.org/10.1016/c2015-0-01032-2

Zhang, Q., & Zhang, Z. (2012). A simplified nonlinear approach for single pile settlement analysis. *Canadian Geotechnical Journal*, *49*(11). https://doi.org/10.1139/T11-110